



# THE NOVEL WOUND-ROTOR HYBRID STEPPING MOTOR

**Jonathan U. Agber<sup>1</sup>     Johnson Mise Akura<sup>2</sup>**

Senior Lecturer, Department of Electrical and Electronics Engineering, University of Agriculture, Makurdi, Nigeria<sup>1</sup>

Lecturer II, Department of Electrical and Electronics Engineering, University of Agriculture, Makurdi, Nigeria<sup>2</sup>

**ABSTRACT:** Hybrid stepping motors can be analyzed as synchronous motors with constant field excitation. One limitation on the operation of these motors is the inability to regulate the permanent magnet (PM) mmf in order to obtain a family of steady state characteristics like conventional synchronous motors. The aim of this paper is to investigate the dependence of the PM hybrid motor characteristics on rotor excitation. Hence the design and construction of a wound-rotor motor, in which the two permanent magnets in the rotor of the hybrid stepping motor were replaced with wound soft iron formers. Static tests with varying rotor mmf were carried out and the results obtained show that the holding torque varies with rotor excitation and also that the PM mmf varies with the stator excitation.

**Keywords:** Hybrid Motor, Stepping Motor, Synchronous Motor, Wound-Rotor Motor, Static Characteristics

## I. INTRODUCTION

Stepping motors are electromechanical incremental actuators, which convert digital pulses into discrete linear or angular motion of precisely defined rotor position (steps) instead of continuous motion as in conventional motors. There are many variations of stepping motors, which are offshoots of the two basic types: variable reluctance (VR) and hybrid. They both have toothed stator and rotor made of magnetically permeable material. The source of flux is a permanent magnet (PM), a current-carrying winding or a combination of the two [1], [2]. Their principle of operation is based on the fact that both the stator and rotor teeth experience equal and opposite magnetic forces, which tend to align them and minimize the air gap [3].

Hybrid stepping motors can be analyzed as synchronous motors with constant field excitation [4]. One limitation on the operation of these motors is the inability to regulate the PM mmf in order to obtain a family of steady state characteristics like conventional synchronous motors. This problem was tackled by constructing a hybrid stepping motor with a ring coil, in which stator laminations were divided into two sections and separated by a ring coil and the PM in the rotor was replaced by a soft iron sleeve [5].

The design of the wound-rotor (WR) motor involved the replacement of the two permanent magnets in the rotor of the PM hybrid stepping motor with wound soft iron formers. The design method used was developed and documented elsewhere [3], [6], [7]. This method involves the calculation of the holding torque of a stepping motor using the permeance functions at aligned ( $P_1$ ) and unaligned ( $P_2$ ) positions at given stator excitation and PM mmf. The basis of design is a commercial PM hybrid stepping motor model VM156-270BK manufactured by G.E.C.

For a suitable choice of PM mmf, the holding torque vs stator current ( $Th / I_s$ ) curve of this motor was estimated. Using this mmf together with the B-H curve of the PM and soft-iron materials, the dimensions and winding parameters of the soft-iron formers to replace the PMs in the rotor stacks were calculated.

The WR hybrid motor used the same components as the PM hybrid motor, but with the PMs replaced with wound soft-iron formers. The aim of this paper is to investigate the dependence of the hybrid motor characteristics on the PM strength. Hence four types of static tests were carried out in which:

- The flux-linkage/rotor angular position characteristics measured from one of the stator bifilar windings at variable rotor excitation and unexcited stator winding (flux-linkage/rotor angular position at zero stator excitation),
- Flux-linkage /rotor angular position  $\varphi(F, \theta)$  characteristics measured at the stator rated current of 15Amps with variable rotor excitation measured using the other stator bifilar winding.



# International Journal of Advanced Research in Electrical, Electronics and Instrumentation Engineering

(An ISO 3297: 2007 Certified Organization)

Vol. 2, Issue 9, September 2013

- c) Holding torque/stator current characteristics measured at variable stator and rotor excitations.
- d) Static torque/rotor angular position characteristics measured at variable stator excitation with variable rotor excitation.

## II. DESIGN CONSIDERATION

The parameter of interest is the PM mmf, which was found from the family of holding torque/stator current ( $Th / I_s$ ) curves at various PM mmfs. The predicted curves were compared with the experimental curve obtained from the PM hybrid stepping motor. The mmf that best modeled the PM hybrid motor  $Th / I_s$  curve was used to calculate the dimensions and winding parameters of the WR motor.

### A. Calculation of holding torque vs stator current characteristics

The holding torque  $Th$  is the peak value of static torque that a motor of given rotor volume can produce at a given stator excitation.

It can be expressed [3], [6], [8], [9] as:

$$Th = K_t K_u K_e T_{ls} V_r \quad (1)$$

where  $K_t$ ,  $K_u$  and  $K_e$  are ratio of peak to mean torque between zeros (shape factor), utilization factor and coefficient of excitation, while  $T_{ls}$  and  $V_r$  are limiting value of specific mean torque and active rotor volume respectively.

$T_{ls}$  can be calculated from known motor geometry and the air gap permeance  $P_1$  and  $P_2$ , with the assumption of a nominal saturation value of flux-density  $B_s = 2.1T$ .

$$T_{ls} = 2 \frac{(B_s t)^2}{\mu_0 \lambda^2} \left( \frac{1}{P_1} - \frac{1}{P_2} \right) \quad (2)$$

$P_1$  and  $P_2$  can be calculated from the  $\varphi / i$  curves for aligned and unaligned positions [8] or interpolated from curves [6] at given  $\lambda / g$  and  $t / \lambda$  (where  $\lambda$ ,  $t$  and  $g$  are tooth pitch, tooth width and air gap respectively). For the motor under consideration,  $P_1$  and  $P_2$  were interpolated from the curves supplied by Harris and Finch [6], with the numerical values of 18.337 and 4.760 respectively.

The shape factor  $K_t$  is found as the ratio of the peak ( $Th$ ) to the mean ( $T_{av}$ ) between successive torque zeros of  $T(i, \theta)$  curves.

$$K_t = \frac{Th}{T_{av}} \quad (3)$$

where

$$T_{av} = \frac{1}{\pi} \int_0^\pi T(i, \theta) d\theta \quad (4)$$

For initial design calculations, the excitation factor  $K_e$  was calculated using the normalized coenergy ( $S$ )/( $F$ ) curves published by Harris and Finch [8]. The critical mmf  $F_c$  and the saturated value of flux per tooth pitch  $\varphi_{ls}$  can be defined as:

$$F_c = \frac{B_s t}{\mu_0 P_2} \quad (5)$$

$$\varphi_{ls} = B_s t L \quad (6)$$

where  $L$  is the active core length. Based on equations 5 and 6, the numerical values of  $F_c$  and  $\varphi_{ls}$  were found to be 801.27At and 0.702mWb respectively.



## International Journal of Advanced Research in Electrical, Electronics and Instrumentation Engineering

(An ISO 3297: 2007 Certified Organization)

Vol. 2, Issue 9, September 2013

Having obtained  $F_c$  and  $\varphi_{1s}$  the  $\varphi/F$  curves were normalized and the normalized coenergy curves were calculated. The excitation factor  $K_e$  was calculated from the normalized coenergy curves at known ( $F$ ) as follows:

$$K_e = (S_1) - (S_2) + (S_3) \quad (7)$$

where  $S_1$  was calculated from the expression derived elsewhere [6]. For doubly excited motors, such as the PM hybrid,  $K_e$  has forward ( $F_f$ ) and backward ( $F_b$ ) normalized mmf components, which were calculated as:

$$(F_f) = \frac{F_m / 2 + F_e}{F_c} \quad (8)$$

$$(F_b) = \frac{F_m / 2 - F_e}{F_c} \quad (9)$$

where  $F_m$ ,  $F_e$  and  $F_c$  are PM, stator winding and critical mmfs respectively.

From ( $F_f$ ) and ( $F_b$ ), the corresponding ( $S_2$ ) and ( $S_3$ ) could be interpolated from the ( $S$ )/( $F$ ) curves [3]. The utilization factor  $K_u$  represents the fraction of the whole rotor that is effectively utilized for torque production, with the excitation pattern appropriate to any one step [6], [10]. For the present case, one-phase excitation was used and  $K_u$  was estimated as:

$$K_u = K_\varphi \frac{N_{se}}{N_r} = 0.4K_\varphi \quad (10)$$

where  $K_\varphi$ ,  $N_r$ , and  $N_{se}$  are phase spread factor within  $K_u$ , number of rotor teeth and number of excited stator teeth respectively.

Based on previous designs [6], [9], a value of  $K_\varphi = 0.625$  was chosen.

Having obtained all the necessary coefficients and motor dimensions, a computer program for the prediction of  $Th / I_s$  was developed to handle this task. The measured and predicted  $Th / I_s$  curves at various PM mmfs were plotted, from which the  $Th / I_s$  curve at  $F_r = 600At$  was found to be the best approximation of the PM hybrid motor.

### B. Calculation of soft-iron former dimensions

Having established the PM mmf, the dimensions of the soft-iron former (flux carrier) on which the rotor windings would be wound were calculated. The PM dimensions are shown in Table 1.

Using these dimensions and the B-H curve of the magnetic material (ALCOMAX II) published in a bulletin [11], the magnetic flux  $\varphi_m$  was calculated.

For the calculation of the dimensions of the soft-iron former, it was assumed that the soft-iron former should be capable of carrying  $\varphi_m$  with a drop not exceeding 7.5% of the winding mmf. Using this as a guide, the soft-iron material to replace the PM was chosen. The choice of MAXIMAG was based on the fact that it is a commercially available soft-iron material, whose magnetic characteristics are similar to silicon steel with which the stator and rotor laminations of the hybrid motor were made. From the 7.5% mmf drop, the field strength  $H_i$  and the flux-density  $B_i$  of the soft-iron material were calculated using the MAXIMAG B-H curve.

The cross-sectional area of the soft-iron former ( $A_i$ ) was calculated as.

$$A_i = \frac{\varphi_m}{B_i} \quad (11)$$

The other dimensions of the soft-iron former were calculated with allowance for end-cheeks. These dimensions are displayed in Table 1.

The cross-sectional view of the soft-iron former is shown in Figure 1. Having obtained the needed dimensions, the end-cheeks were checked for saturation and  $t_c$  was adjusted to 3.4mm.

# International Journal of Advanced Research in Electrical, Electronics and Instrumentation Engineering

(An ISO 3297: 2007 Certified Organization)

Vol. 2, Issue 9, September 2013

Table 1: The dimensions of the PM and WR former

Parameters	Motor	PM	WR
Outer diameter (mm)		$D_{om} = 70.86$	$D_{of} = 70.86$
Inner diameter (mm)		$D_{in} = 32.55$	$D_{if} = 28.0$
Length (mm)		36.05	36.05
Height of end-cheeks (mm)		-	$t_c = 3.00$
Thickness of end-cheeks (mm)		-	$h_c = 4.30$

### C. Calculation of winding parameters

The cross-sectional area (csa) of the winding  $A_w$  was calculated from the soft-iron and PM dimensions as:

$$A_w = 0.5(D_{om} - D_{of})(L_m - 2t_c) \quad (12)$$

Having obtained  $A_w$ , the calculation of the winding parameters was carried out. This involved the calculation of the number of turns  $N_w$ , the winding resistance  $R_w$ , the current density  $J_w$  and power dissipation.

For the calculation of  $N_w$ , a packing factor  $K_p = 0.73$  was assumed and used to estimate the copper area  $A_{cu}$ .

$$A_{cu} = A_w K_p \quad (13)$$

$N_w$  is the ratio of  $A_{cu}$  and the csa of standard copper wires  $W_{csa}$ .

$$N_w = \frac{A_{cu}}{W_{csa}} \quad (14)$$

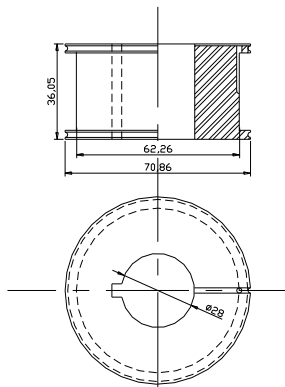


Figure 1. The soft-iron former to replace the permanent magnet

To estimate the resistance of the winding, the length of a mean turn  $L_{mt}$  was calculated.

$$L_{mt} = \pi(D_{om} - D_{of}) \quad (15)$$

The resistance of the winding was then calculated from the expression:

$$R_w = N_w L_{mt} \sigma \quad (16)$$

where  $\sigma$  is the resistance of copper wire per metre at 20°C. Using  $F_m$ ,  $W_{csa}$  and  $N_w$ , the current and current-density for selected diameters of copper wires were estimated. For the calculation of the rise in temperature  $dy/dt$ , it was assumed that no heat would be dissipated, i.e. the whole heat would be retained in the winding. For this case it can be shown that

$$\frac{dy}{dt} = \frac{J_w^2 \rho}{\delta_c C_p} \quad (17)$$

where  $\rho = 1.8E-05$  Ohm m - resistivity of copper at 20°C



# International Journal of Advanced Research in Electrical, Electronics and Instrumentation Engineering

(An ISO 3297: 2007 Certified Organization)

Vol. 2, Issue 9, September 2013

$\delta_c = 8.96e^{-03} \text{ Kg / m}$  - density

$C_p = 0.39 \text{ KJ/(Kg K)}$  - specific heat.

The voltage drop and power dissipation in the winding were then estimated.

The choice of wire was influenced by the dc power source and the heating constraint. Based on the above, a grade 2, class H wire with  $d_{nom} = 0.56\text{mm}$  was chosen.

### III. CONSTRUCTION OF THE MOTOR

The soft-iron formers to replace the PMs were constructed from the commercial material MAXIMAG as shown in Figure 1. A groove was provided in each end-cheek to accommodate a search coil for measurement of rotor flux. Other grooves and holes were made to carry the winding leads, and a key-way was provided so that the formers could be secured to the rotor shaft. The constructed soft-iron formers were wound with 240 turns of 0.56mm, grade 2, class H wire with a packing factor  $K_p = 0.55$  ( $K_p$  was reduced due to slot liner).

The motor components (wound stator, rotor end-cups, shaft and keys) were supplied by GEC. These components were of the same profile as those used in the PM hybrid stepping motor model VM 156-270BK. The stator, which had eight poles, had two windings on each pole. The start and finish of each winding were clearly marked, thus enabling different stator winding connections to be adopted.

The normal hybrid shaft required some modifications, which included:

- the provision of a second groove through which the wound-rotor leads could pass to the non-drive end,
- the non-drive end had to be machined down to remove the end-cup stopping stub, which was replaced with a ring and a retaining pin,
- provision had to be made for mounting slip-ring assembly.

Having made the above modifications, the rotor was assembled with an aluminium disc separating the two stacks. The rotor was then ground to size.

The assembled rotor underwent heat test, in which the series connected rotor windings were subjected to a constant current of 2.5A, corresponding to 600At. The required voltage was recorded at minute intervals. The rise in temperature was calculated from the increase in resistance method. As the current was kept constant at 2.5A, it was not possible to reach the final temperature. However, the rate of rise of temperature with time, the initial and final temperatures were found by extrapolation.

The measured and calculated winding parameters of the 0.56mm copper wire are shown in Table 2. Although this test was carried out with the rotor exposed in the air, satisfactory results were obtained. These results gave indication on the duration the rotor winding could be subjected to the rated current without any deterioration in the insulation. It was established that a rise of 60°C occurred in 30 minutes, which clearly showed that under normal conditions, the motor could be safely tested for more than 30 minutes.

Table 2: Measured and calculated winding parameters for the soft-iron former

$D_{nom}=0.56\text{mm}$ , Grade 2, Class H	N turns	R at 0°C Ohms	R at 120°C Ohms	I A	V at 0°C V	V at 120°C V	$J_w$ A/mm	$d\gamma/dt$ °C/min
Design calculations	292	4.24	6.43	2.05	8.69	13.18	6.55	13.28
Final measurements	240	3.73	4.92	2.50	9.33	12.30	10.55	12.35

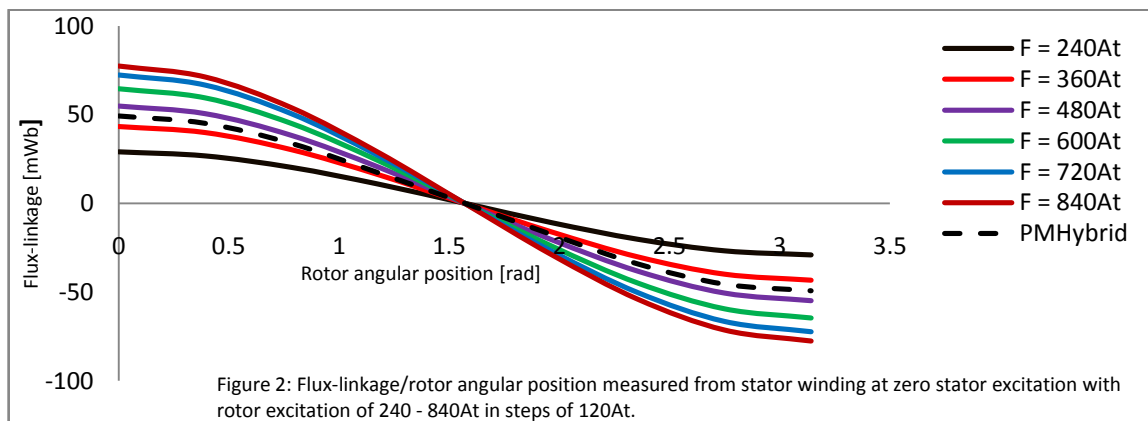
The slip-ring and brush assembly were constructed and the whole WR hybrid stepping motor was assembled. The two rotor windings were connected in series, such that when excited, the rotor stacks formed a magnetic circuit consisting of N-S-N-S poles, as in the case for the PM hybrid rotor. The rotor search coils were also connected in series, so that the total flux from the two rotor stacks could be measured.

## IV. STATIC TESTS

The static test rig and test procedure were similar to those described by Agber [12]. For the static tests, the stator windings were connected in the same way as the PM hybrid motor, with phase A connected to the dc supply, while phase C was connected to the flux-meter. The static rig was modified by providing a power supply unit for the rotor winding. The test procedure was the same with the PM hybrid motor. Four static tests were carried out:

- The flux-linkage/rotor angular position characteristics measured from one of the stator bifilar windings at variable rotor excitation and unexcited stator winding (flux-linkage/rotor angular position at zero stator excitation) – Figure 2,
- Flux-linkage /rotor angular position  $\varphi(F, \theta)$  characteristics measured at the stator rated current of 15Amps with variable rotor excitation using the other stator bifilar winding (Figure 3).
- Static torque/rotor angular position characteristics measured at variable stator excitation with variable rotor excitation. Holding torque/stator current characteristics measured at variable stator and rotor excitations (Figure 4).
- Holding torque/stator current characteristics measured at variable stator and rotor excitations (Figure 5).

These tests are necessary because they provide a means by which the flux and static torque curves of the PM and WR hybrid motors can be directly compared, with a view of estimating the PM working point at various stator excitations.



## V. DISCUSSIONS

These tests provided a means for comparing the PM hybrid motor with its WR counterpart.

Figure 2 are plots of flux-linkages/rotor angular position for both the PM and WR hybrid motors measured from one of the stator bifilar windings at zero stator excitation. The flux-linkage curve for the PM hybrid motor lies between those of the WR motor measured at  $F_r = 360\text{At}$  and  $F_r = 480\text{At}$ . The plots also show that as the rotor mmf is varied, the change in magnitude of the flux-linkage curves is not proportional to the change in rotor mmf, showing some form of saturation at higher rotor mmfs.

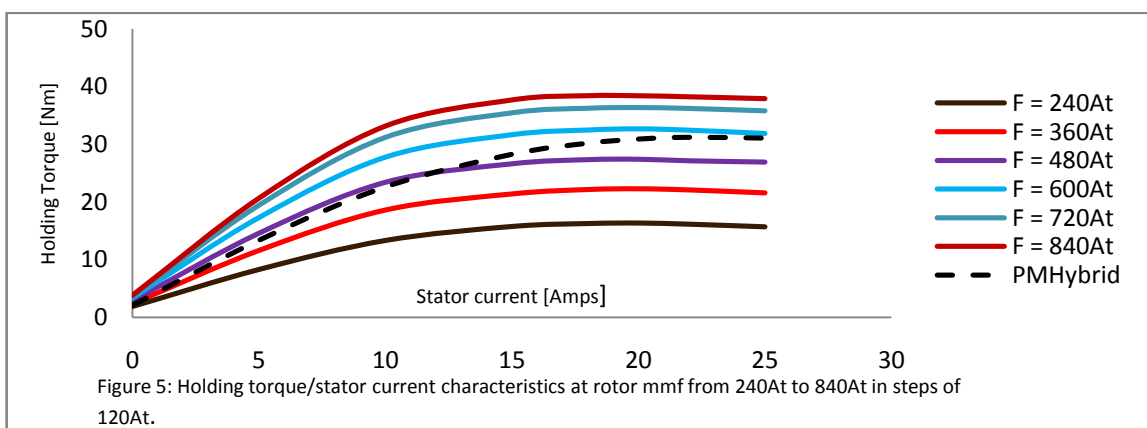
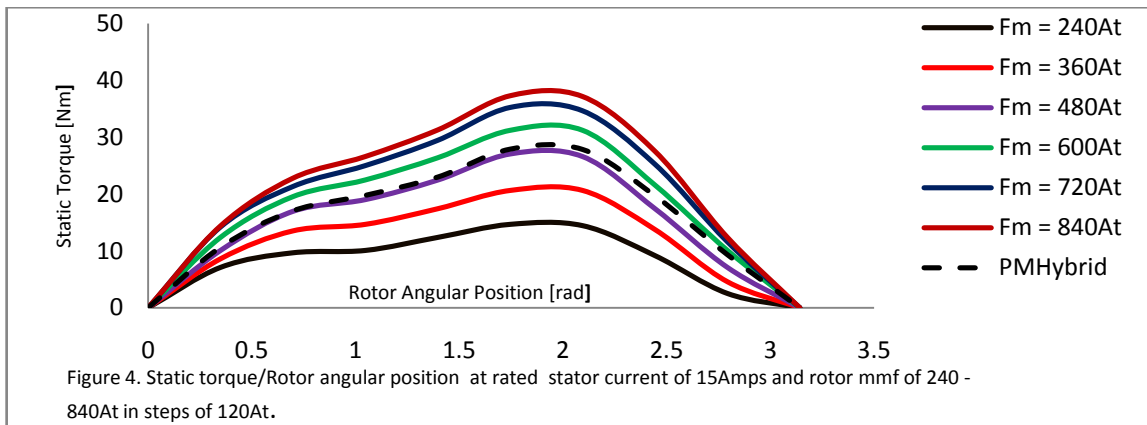
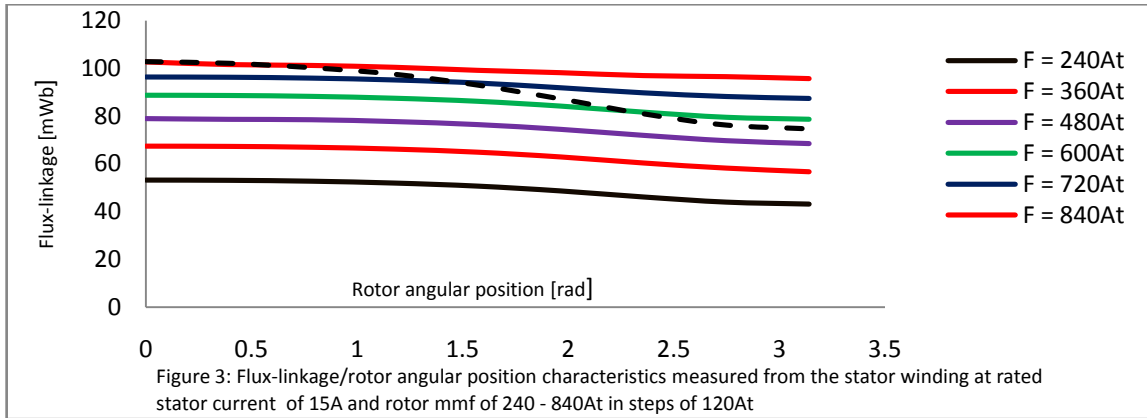
Figure 3 is the flux-linkage/rotor angular position for both the PM and WR hybrid motors measured from one of the bifilar windings, while the other is energized at twice the motor rated current with the WR rotor mmf varied from  $F_r = 240\text{At}$  to  $840\text{At}$  in steps of  $120\text{At}$ . The following observations are derived:

- At  $\theta = 0$ , the numerical values of flux-linkage for the PM hybrid motor and the WR at  $F_r = 840\text{At}$  are approximately equal.
- As the rotor angular position changes from  $\theta = 0$  to  $\theta = \pi$ , the PM flux-linkage curve varies, crossing the WR curves for  $F_r = 720\text{At}$  and  $F_r = 600\text{At}$  respectively.

# International Journal of Advanced Research in Electrical, Electronics and Instrumentation Engineering

(An ISO 3297: 2007 Certified Organization)

Vol. 2, Issue 9, September 2013



iii) At  $\theta = \pi$ , the PM hybrid motor flux-linkage curve settles between the WR motor curves at  $F_r = 600\text{At}$  and  $F_r = 480\text{At}$ .

An extension of these  $\varphi(F, \theta)$  characteristics to other stator currents, say 5, 10 and 20Amps will show varying dependence of PM flux on rotor excitation.

Figure 4 displays the static torque vs rotor angular position characteristics of both motors at the stator rated current of 15Amp. It can be seen that the PM hybrid motor characteristic lies between those of the WR motor at  $F_r = 480$  and  $600\text{At}$  but closer to the WR characteristic at  $F_r = 480\text{At}$ .



# International Journal of Advanced Research in Electrical, Electronics and Instrumentation Engineering

(An ISO 3297: 2007 Certified Organization)

Vol. 2, Issue 9, September 2013

Figure 5 contains plots of holding torque against stator current ( $T_h / I_s$ ) for both PM and WR hybrid motors. The WR hybrid motor plots are done for rotor excitations of  $F_r = 240\text{At}$  to  $F_r = 840\text{At}$  in steps of  $120\text{At}$ . The following observations are derived:

- i) At zero stator current, the cogging torque of the PM hybrid motor lies between those of  $F_r = 240\text{At}$  and  $360\text{At}$ .
- ii) As the stator current is increased, the PM hybrid motor holding torque curve moves away from its initial position and lies between the WR motor curves for  $F_r = 360$  and  $480\text{At}$  and cuts the WR motor curves for  $F_r = 480\text{At}$ ,  $600\text{At}$  and settles close to the curve of  $F_r = 600\text{At}$ .
- iii) The holding torque for the PM hybrid stays fairly linear for the range of current covered, unlike the WR hybrid.
- iv) The WR hybrid motor characteristics saturate faster than that of the PM hybrid.

## VI. CONCLUSION

Figure 3 is the  $\varphi(F, \theta)$  characteristics of the PM and WR hybrid motors. It shows the dependence of PM flux on rotor mmf. An extension of the  $\varphi(F, \theta)$  characteristics to other values of stator current will show further dependence of PM mmf on stator excitation.

Figure 5 shows the holding torque characteristics of the PM and WR hybrid motor as the stator current is varied from zero to 25Amps and the stator mmf varied from  $F_r = 240\text{At}$  to  $F_r = 840\text{At}$  in steps of  $120\text{At}$ . It shows how the holding torque characteristic of the PM hybrid motor rises steadily from the initial value of  $I_s = 0$  to the final value of  $I_s = 25\text{Amps}$ . It also shows how the holding torque curve of the PM hybrid motor cuts the WR motor torque curves of  $F_r = 360\text{At}$  and  $480\text{At}$  and finally settling between  $F_r = 480\text{At}$  and  $600\text{At}$ , as it transverses from  $I_s = 0$  to  $I_s = 25\text{Amps}$ . These  $T_h / I_s$  curves also show that the PM mmf in the PM hybrid stepping motor varies with variation in stator current.

It has been established in Figures 3 and 5 that the PM mmf in the PM hybrid stepping motor varies as the stator excitation varies. Hence with the possibility of regulating the rotor mmf of the WR hybrid stepping motor, a family of characteristics similar to those of conventional synchronous motors can be produced.

## REFERENCES

- [1] P. Acarnley, "Stepping Motors: A Guide to Theory and Practice", IET Control Engineering Series 63, 4<sup>th</sup> Ed. The Institution of Engineering and Technology, London, UK., 2007.
- [2] V. V. Athani, "Stepper Motors: Fundamentals, Applications and Design", New Age International (P) Ltd., 2005.
- [3] Finch, J. W. and Harris, M. R. "Linear Stepping Motors: An Assessment of Performance", *Proc. Int. Conf. on Stepping Motors*, University of Leeds, pp 24 – 31, 1979.
- [4] Snowden, A. E. and Madsen, E. W. "Characteristics of a Synchronous Inductor Motor", *Trans. AIEE Application and Industry*, Vol. 81, pp 1 -5, 1962.
- [5] Kuo, B. C and Ward, D. "A Hybrid Stepping Motor With a Ring Coil", *Proc. 10<sup>th</sup> Annual Symposium on Incremental Motion Control Systems and Devices*, University of Illinois, pp 169 – 176, 1981.
- [6] Harris, M. R. and Finch, J. W. "Estimation of Static Characteristics in hybrid Stepping Motors", *Proc. 8<sup>th</sup> Annual Symposium on Incremental Motion Control Systems and Devices*, University of Illinois, pp 293 – 306, 1979.
- [7] Finch, J. W., Harris, M. R. and Musoke, A. "Normal Forces in Linear Stepping Motors" *IEE Conf. Publication on Small and Special Electric Machines*, No. 202, pp 78 – 81, 1981.
- [8] Harris, M. R., Hughes, A. and Lawrenson, P. J. "Static Torque Production in Saturated Doubly – Salient Machines", *Proc. IEE*, Vol. 122, No. 10, pp1121 – 1127, 1975.
- [9] Harris, M. R., Andjargholi, V., Lawrenson, P. J., Hughes, A. and Ertan, B. "Unifying Approach to the Static Torque Production of Stepping – Motor Structures" *Ibid*, Vol. 124, No. 12, pp 1215 – 1224, 1977.
- [10] Krishnan, R. "Switched Reluctance Motor Drives – Modeling, Simulation, Analysis, Design and Application" Industrial Electronics Series, CRC Press LLC, Boca Raton, Florida 3343, 2001.
- [11] The Sheffield Magnetic Co. Ltd. "Technical Bulletin on Magnetic Properties and Design Data for Standard P.M.A. Materials" No. 1, 12, 1967.
- [12] Agber, J. U. "Analysis of Detent Torque in Hybrid Stepping Motors", *International Journal of Engineering and Science (IJES)*, Vol. 2, issue 5, pp. 35 – 41, 2013.